On Passive Quadrupedal Bounding with Translational Spinal Joint*

Konstantinos Koutsoukis and Evangelos Papadopoulos

Abstract— This paper studies the effect of a flexible linear torso on the dynamics of passive quadruped bounding. A reduced-order passive and conservative model with translational spinal joint and springy legs is introduced. Numerical return map studies reveal the existence of a confined area of fixed points generating high-speed cyclic bounding motions by exploiting the natural dynamics of the model. The corresponding motion features extensive bidirectional spine deformation. The model displays interesting techniques that result in high-speed locomotion, such as increased flight phase duration and stride length. The obtained results show that the corresponding robot gaits and the associated performance resemble those of its natural counterparts even though the spinal joint lies beyond the bioinspired regime.

I. INTRODUCTION

During the last forty years, research endeavors related to legged robots have spawned a large number of impressive robots, starting from Raibert's pioneering robots [1] and reaching up to contemporary ones such as the Spot [2], the MIT Cheetah [3], the HyQ [4] and the Starleth [5]. Quadruped robots demonstrate increased versatility and mobility in contrast to wheeled robots. Notwithstanding these benefits, legged systems are characterized by high complexity and coupling between the large number of degrees of freedom. To address this issue, a diverse set of simplified dynamic models has been introduced to capture the dominant features of legged locomotion.

The Spring Loaded Inverted Pendulum (SLIP) [6], set the stage for the vast majority of the subsequent quadruped models. The first quadruped model introduced by Nanua [7], was composed of a rigid body and two massless springy legs. The model was passive and conservative, and was able to perform a number of gaits (trot, bound, gallop). Subsequent studies with this model focused on the passive self-stable bounding generated by exploiting the natural dynamics [8]. The rigid torso model was successfully employed in control schemes for dynamically stable quadrupedal locomotion with moderate speeds [9].

Aiming to high-speed robots, engineers looked for inspiration at their natural counterparts and the features they possess. The flexible torso is considered a key feature to attaining high velocities. According to studies focusing on biological data, the extensive deformation of the flexible torso has a great contribution in increasing stride length [10], [11] (see Fig.1) while the stride frequency remains roughly constant [12]. In addition, the flexible torso enhances energy efficiency by storing the fluctuating energy due to the swinging of a quadruped leg at elastic musculature elements of the spine. Based on these biological findings a new generation of quadruped robots, featuring various flexible torso designs has been developed [3], [12]-[15].
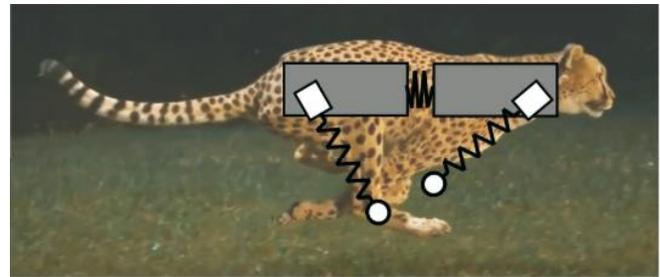

Figure 1.   The sagittal model with a flexible linear spine overlayed a cheetah at the *gathered flight phase* in the background.

Since the rigid torso model could not address torso flexibility, new simplified dynamic models were proposed in order to permit an insight to the effect of spine motions in quadruped locomotion. A passive model with a revolute spinal joint modeled as a torsional spring, and with massless springy legs was introduced [16]. The model could yield cyclic bounding motions in a reduced gravity environment. Numerical return map studies in a dimensionless setting, lead to a self-stable, passively realized bounding motion for certain combinations of torso and leg compliance [17]. Bounding gait was also studied using a quasi-passive model with a revolute spinal joint controlled by a locking mechanism [18], and non-trivial two-segment legs [19] whereas other approaches implied actuated torso joints [20].

As one can observe easily, the morphology of the spine of mammals prompted the vast majority of researchers to propose models incorporating spinal revolute joints. However, the already proposed models cannot capture the extensive length variation during high-speed galloping observed in nature, as for example in the cheetah, see Fig. 1.

In this work, we introduce a sagittal plane model with a translational (linear) flexible torso and massless springy legs, for the first time in the literature, to the best of our knowledge. The model is passive and conservative. Despite its simplicity, it allows the prediction of the existence of repetitive passive gaits corresponding to Poincaré fixed-points, and of resulting motions resembling those of its natural counterparts. The developed model is the only one that captures the extensive variation of the sagittal hip-to-hip distance due to spine deformation. This property has not been captured in other works so far, due to the use of a revolute spinal joint.

The structure of the paper is as follows. In Section II, the model with the flexible linear torso is introduced and the phases and transitions of bound gait are presented. Section III discusses in detail the main properties of the calculated cyclic bounding motions realized passively. Section IV concludes the paper.

II. BOUNDING WITH A TRANSLATIONAL SPINAL JOINT

A quadruped robot is a complex nonlinear system, characterized by hybrid dynamics and by a strong coupling between its many degrees of freedom. To study the effect of the flexible linear torso during fast locomotion, a simplified sagittal model of a quadruped robot is introduced, see Fig. 2.

A. Model description and parameters

The main body of the model consists of two segments (hind and fore segment). The two segments of the body are connected via the spinal translational joint, which is passive. A linear spring connects the two body segments and allows no rotation between them. Two springy legs are connected to each of the two body segments at the hips with revolute joints. The choice of springy legs is in analogy with the Spring Loaded Inverted Pendulum (SLIP) and captures the property of energy storage during running. Subscripts f, h, and t, refer to the fore and hind individual body segments (or legs) and to the torso, respectively.

As far as the dynamics of the model is concerned, the hind and fore segments of the body are identical with mass m and moment of inertia I_z about their center of mass (CoM). The legs are massless springs of nominal length L and spring stiffness k, and the distance between the hip joint and the CoM of each body is d. The spinal linear spring has stiffness k_t and nominal length L_t.

The model is conservative since energy dissipation and motor torques are not considered. The model parameters are chosen to match those in [21]. The value for the stiffness of the torso linear spring was chosen so that the herein introduced model and the model of [21] have the same natural frequency. The mechanical properties are displayed in Table I.
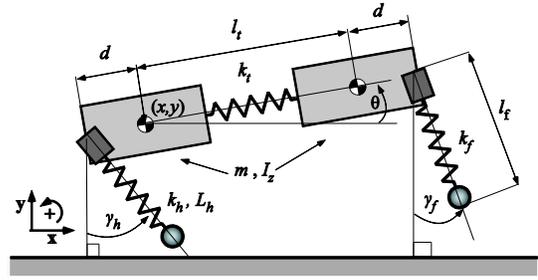

Figure 2.   The sagittal-plane model of a quadruped robot with a translational (linear) spinal joint.

TABLE I. MODEL MECHANICAL PROPERTIES

PARAMETER	VALUE	UNITS
Fore/Hind Body Mass (m)	10.432	kg
Fore/Hind Body Inertia (I_z)	0.339	kg m^2
Hip to CoM distance (d)	0.138	m
Nominal Leg Length (L)	0.323	m
Leg Spring Constant (k)	7046.0	N/m
Nominal Torso Spring Length (L_t)	0.276	m
Torso Spring Stiffness (k_t)	5077.0	N/m

B. Bounding gait description

In nature, mammals use their spine mainly during high speed galloping [10], [11], [22]. Galloping is an asymmetric gait, featuring great complexity since none of the legs moves in phase. Instead bounding, i.e. the gait at which the fore and the hind legs move in phase, is easier to model and is employed frequently in nature during obstacle avoidance and running with moderate speed. Bounding has received considerable attention due to its sagittally symmetric nature and to its use as a limiting case of galloping. Here, we study the spine performance during bounding, see Fig.3.
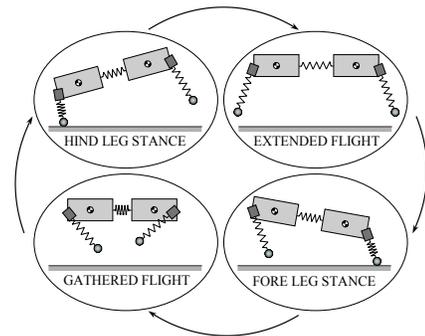

Figure 3.   Bounding phases

Bounding consists of four phases, two aerial and two stance phases triggered by events such as leg liftoff and leg touchdown. It is interesting to note the existence of two flight phases. During the *gathered flight phase*, the spine spring reaches its minimum length, letting the two body segments to approach. No collision is modeled, so the two

CoMs can come as close as needed. During the *extended flight phase*, the spinal spring reaches its maximum length, increasing the distance between them.

The existence of a fifth phase, called *double stance phase*, during which the two legs are in contact with the ground simultaneously, is also possible. In such a case, the double stance replaces the gathered flight phase; however this type of bounding is not studied here.

C. Equations of motion

The equations of motion are derived using the Lagrangian formulation. Virtual legs, i.e. the fore or hind leg pairs that move together, are used to replace these pairs by a single leg of double stiffness. The generalized coordinates include the Cartesian coordinates of the CoM of the hind segment (x, y), the pitch angle θ of the body and the spinal spring length l_t i.e. the distance between the CoMs of the two body segments.

Defining as $\mathbf{q} = [x \quad y \quad \theta \quad l_t]^T$, the equations of motion can be written in matrix form as:

$$\mathbf{M(q)\ddot{q}} = \mathbf{F(q,\dot{q})} + \mathbf{G(q)} \tag{1}$$

where

$$\mathbf{M(q)} = \begin{bmatrix} 2m & 0 & -ml_t\sin\theta & m\cos\theta \\ 0 & 2m & ml_t\cos\theta & m\sin\theta \\ -ml_t\sin\theta & ml_t\cos\theta & 2I_z + ml_t^2 & 0 \\ m\cos\theta & m\sin\theta & 0 & m \end{bmatrix} \tag{2}$$

$$\mathbf{F(q,\dot{q})} = \begin{bmatrix} 2m\dot{\theta}\dot{l}_t\sin\theta + m\dot{\theta}^2 l_t\cos\theta + F_h\sin\gamma_h + F_f\sin\gamma_f \\ -2m\dot{\theta}\dot{l}_t\cos\theta + m\dot{\theta}^2 l_t\sin\theta + F_h\cos\gamma_h + F_f\cos\gamma_f \\ -2m\dot{\theta}\dot{l}_t l_t + F_f(d+l_t)\cos(\theta-\gamma_f) - F_h d\cos(\theta-\gamma_h) \\ k_t(L-l_t) + m\dot{\theta}^2 l_t + F_f\sin(\theta-\gamma_f) \end{bmatrix} \tag{3}$$

and the vector $\mathbf{G}$ contains the gravitational terms.

D. Events and phase transition

The dynamics of the model is hybrid, containing terms that are activated and deactivated depending on the phase of bounding. Of major importance are the conditions under which an event occurs and triggers the phase transition for the model. The touchdown and liftoff events, as well as the phase transitions are described below.

1) Touchdown events: The flight phase terminates when the lower part of the leg touches the ground. Using the absolute angles (γ_f, γ_h) of the leg and Cartesian coordinates of the hind segment of the body, the criterion for the touchdown event to occur for the hind leg is:

$$y - d\sin\theta - L\cos\gamma_h = 0 \tag{4}$$

Accordingly, the criterion of the fore leg touchdown is:

$$y + (d+l_t)\sin\theta - L\cos\gamma_f = 0 \tag{5}$$

2) Liftoff events: The stance phase terminates when the ground reaction force becomes zero and the leg acceleration is positive i.e. the leg and consequently the segment to which it is attached is moving upwards. Under the assumption of massless legs, the liftoff threshold is significantly simplified, since the liftoff occurs when a spring leg reaches its nominal length. The threshold function for the fore leg liftoff is:

$$l_f - L = 0 \tag{6}$$

Accordingly, the liftoff criterion for the hind leg is:

$$l_h - L = 0 \tag{7}$$

E. Bounding cyclic motions

To study the existence of bounding cyclic (repetitive) motions as shown in Fig. 3, the Poincaré return map method is employed. The Poincaré section is taken during the extended flight phase at the apex height of the spinal joint, where the vertical velocity of the CoM of the total body (consisting of the two segments) is zero, that is:

$$2\dot{y} + \dot{l}_t\sin\theta + \dot{\theta}l_t\cos\theta = 0 \tag{8}$$

To study the periodic motions through the computations of *fixed-points* on a Poincaré map, the monotonically increasing horizontal coordinate x of the CoM of the hind segment of the body will be projected out of the state vector. A further dimensional reduction inherent to the Poincaré method can be employed to substitute $\dot{y}$, θ and $\dot{l}_t$. The reduced Poincaré map can be defined through the rule,

$$\mathbf{z}[k+1] = \mathbf{P}(\mathbf{z}[k], \mathbf{a}[k]) \tag{9}$$

where

$$\mathbf{z} = (y, \dot{\theta}, \dot{x}, l_t)^T \tag{10}$$

$$\mathbf{a} = (\gamma_f, \gamma_h)^T \tag{11}$$

The leg angles are controlled kinematically during the flight phases, i.e. their values are set and obtained immediately..

III. PASSIVE PERIODIC MOTIONS

In this section, the search method for the passively generated fixed points and the main characteristics of the passively generated motion are presented. The objective of the search scheme is to find an argument $\mathbf{z}_f$ that maps onto itself, i.e. the solution to the equation

$$\mathbf{z}[k+1] - \mathbf{P}(\mathbf{z}[k], \mathbf{a}[k]) = 0 \tag{12}$$

The search for fixed points was conducted in two levels. At the first level, possible areas of existence of fixed points were found, based on a rough search of the initial conditions. At the second level, an extensive search on the specified areas was conducted using MATLAB's *fmincon* and *patternsearch*. The results were filtered to discard from the set of the calculated fixed points, the motions featuring a

double stance phase, since the resulting motion would have been in contrast to the bounding gait described in Section II.

A. Distribution and characteristics of fixed points

Following the aforementioned method, a large amount of fixed points has been calculated. The numerical calculation of the fixed points was a challenging task since they lie in a very confined area. The fixed points on the Poincaré section taken in the extended flight phase at the apex height of the spinal joint are depicted in Fig. 4.
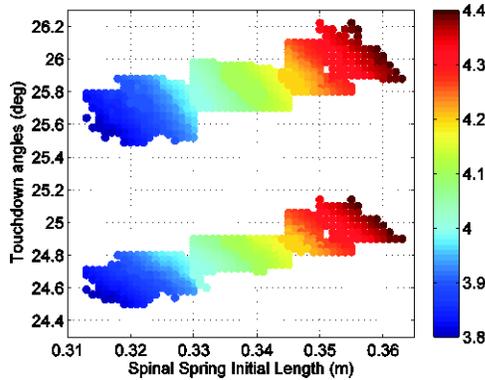

Figure 4. Bounding fixed points for horizontal velocities varying from 3.8 m/s to 4.4 m/s. The vertical axis corresponds to the absolute touch down angles of the hind (lower branch) and the fore leg (upper branch). The horizontal axis corresponds to the initial maximum spinal spring length. The fixed points are colored according to the initial horizontal velocity.

The calculated fixed points exhibit a number of features worth mentioning. Their small amount indicates that the passive model with the translational spinal joint is sensitive and only relatively limited combinations of proper initial conditions and touchdown angles can generate cyclic motions. As shown in Fig. 4, the absolute touchdown angles of interest are located between 24.4 and 26.4 deg., only. The energy distribution among the motion modes for fixed points with different horizontal velocities, give a more clear insight (see Fig 5). Only the energy stored at the spinal spring, which is directly connected to the spine oscillation, changes significantly as the initial horizontal velocity (horizontal velocity at the apex height of the spinal joint) increases, whereas the rotational kinetic, vertical kinetic and gravitational are kept constant.

The small range of fixed points that are associated with the model with the translational spinal joint, presented for the first time in this paper, differs from the wide range of fixed points associated with the revolute spinal joint model [21]. Here, the spine oscillation and forward velocity are so closely related that extremely limited velocity regulation can be achieved within a specified total energy level. The contribution of the absolute touchdown angles of the fore and hind legs to the increase of forward speed is not significant. This fact highlights the importance of the flexible spine despite the relatively low energy related to the torso

oscillations, in comparison with the forward kinetic and the gravitational energy of the system, see Fig. 5.

To gain insight regarding the underlying mechanism implied by the model, and to increase the horizontal velocity, one can focus on the temporal and spatial characteristics of the fixed points during a stride of the cyclic bounding motion. As shown in Figs. 6 and 7, the extensive deformation of the spinal translational joint results in an increase of the stride length, see Fig. 6a. At the same time, the flight phase duration (represented by the sum of gathered and extended flight durations) as well as the torso deformation, both increase as the model attains higher horizontal velocity, Fig. 6b. The stride frequency remains roughly constant since it depends on the dynamic parameters of the model. These observations show that the proposed reduced-order passive model, despite its simplicity, captures the main mechanism for achieving high speeds [22].
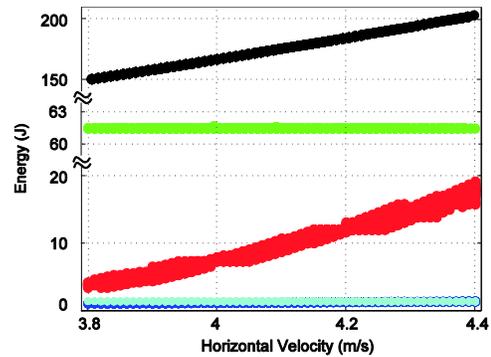

Figure 5. Energy distribution among the modes of the bounding motion for the calculated fixed points. Cyan, blue and black points represent the body segments rotational, vertical and horizontal kinetic energy, respectively. Green points represent the gravitational and red points the spinal spring elastic energy.
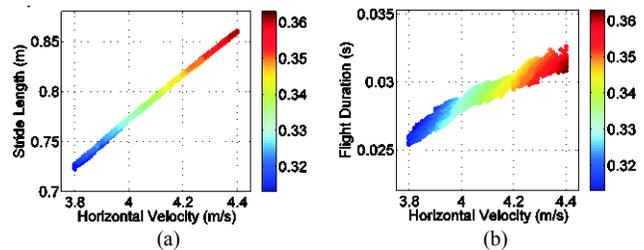

Figure 6. Temporal and spatial characteristics of the calculated fixed points during a stride, with respect to the initial horizontal velocity. (a) Stride length of the calculated fixed points. (b) Flight duration (gathered and extended flight phases) throughout a stride. The points are colored according to the maximum length of the spinal spring during one stride.

B. Main characteristics of the cyclic bounding motions

Despite the different initial conditions and touchdown angles that they exhibit, some basic properties characterize the vast majority of fixed-points. To gain insight on the effect of the flexible linear torso on the bounding motion, we focus next to a representative fixed point. The initial conditions and the touchdown angles of the fixed point are given in Table II.

Figure 7 depicts snapshots of the main events during a stride at the representative fixed point. At the beginning of the stride, the spine spring is extended, the distance between the two body segments has reached its maximum value and the legs have their proper touchdown angles (Fig. 8b). During the extended flight phase, the spine spring is compressed and the initial pitch rate causes the body segments to rotate in the sagittal plane. The free fall terminates when the fore leg touchdown event occurs. During the fore stance phase, the fore leg spring deforms under the impact of the contact force and once it reaches its nominal length again the fore liftoff even occurs (Fig. 9b). The spine spring meets its maximum flexion during the gathered flight phase, and the same sequence of events repeats for the hind legs. At the end of the stride the spine joint reaches its apex high and the spine spring meets its initial length (Fig. 8b).

TABLE II. FIXED POINT INITIAL CONDITIONS AND TOUCHDOWN ANGLES

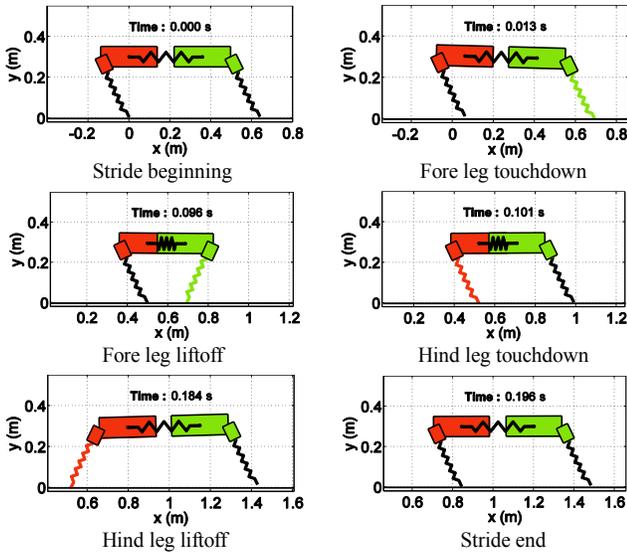| VARIABLE	VALUE	UNITS
Horizontal Velocity of hind body CoM $(\dot{x})$	4.36	m/s
Vertical Position of hind body CoM (y)	0.3	m
Pitch Rate $(\dot{\theta})$	-118.5	deg/s
Spine Spring Length (l_t)	0.359	m
Fore Leg Touchdown angle (γ_f)	25.9	deg
Hind Leg Touchdown angle (γ_h)	24.9	deg

Figure 7. Snapshots of the model's motion during a stride at a representative passively generated fixed point in MATLAB. Fore (hind) leg springs are colored green (red) during fore (hind) stance phase and black during flight phases.

Figure 8 illustrates the time evolution of the horizontal velocity and the spinal spring length throughout a stride of the cyclic motion corresponding to the representative fixed point. Figure 9 depicts the time evolution of the main leg parameters (leg touchdown angle and leg length).
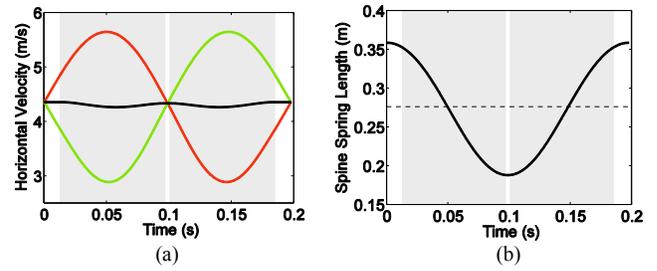

Figure 8. Time evolution of the (a) horizontal CoM velocity of fore (solid green), hind body segment (solid red) and whole system (solid black) and the (b) spine spring length at a representative passively generated fixed point during bounding. The horizontal dashed black line corresponds to the nominal length of the spine spring. Gray areas correspond to fore and hind stance phases.
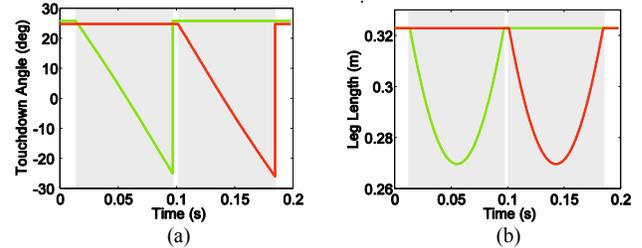

Figure 9. Time evolution of the (a) absolute leg touthdown angles and (b) leg lenth. Green and red lines correspond to fore and hind legs respectively. Gray areas correspond to fore and hind stance phases

The evolution of the vast majority of the main variables of the model with respect to time is qualitatively identical to the results of the rigid torso model presented in [8]. However it is of importance to observe the extensive bidirectional deformation of the spine spring, which leads to a vast change of the overall body dimensions of the model. This characteristic is with complete accordance with the extensive body length variation during high-speed galloping of mammals [10], [11]. To the best of our knowledge, the herein introduced model with the translational spinal joint is the first that exhibits this biomimetic feature. As far as the maximum spinal flexion and extension timing is concerned, they occur before and after hind and fore touchdown events respectively and are not strictly coupled to the events, as described also in the research on therian mammals [23].

In addition, the aforementioned spine deformation is responsible for the large differences between the forward velocity of the fore and hind body segment, while the horizontal velocity of the system CoM remains almost constant during the stride (see Fig. 8a). This difference causes a large deceleration to the body segment in contact with the ground, i.e. during the fore (hind) stance, the fore (hind) body segment is decelerated by the spine. This deceleration results in small leg angular velocities, it increases the stance phases, and decreases the gathered flight phase. This feature is unique in the literature and differs from the revolute spinal joint in [17]. However a slight increase in the duration of the stance phase during high-speed locomotion

has been observed between transverse and rotary gallop, i.e. between galloping with moderate and high speed [22].

In terms of energy efficiency, the herein introduced model seems to have an advantage when compared to the revolute flexible torso model. The advantage comes from the small angular velocities of the legs in contact with the ground, which lead to a restricted leg recirculation during flight. However this advantage can be quantified with non-dimensional analysis similar to the one conducted in [17].

Careful inspection of Fig. 7a reveals that the evolution of the horizontal velocity of the fore body segment, forward in time, is indistinguishable from the evolution of horizontal velocity of the hind body segment. Symmetry can be found also between the fore and hind leg touchdown and liftoff angles, where the absolute touchdown angle of the fore leg equals to the negative of the absolute liftoff angle of the hind leg, see Fig. 8a. The aforementioned time-reversal symmetry is a byproduct of the model symmetric properties of fixed points for the energy-preserving system, and also exists in the rotational spine model [17].

IV. CONCLUSION AND FUTURE WORK

In this paper, the effect of a linear flexible torso during high-speed galloping was investigated by introducing a planar reduced model featuring a translational flexible spinal joint. Passive cyclic motions were discovered and calculated using the Poincaré return map. The fixed points of the model lie on a relatively small range on initial conditions and touchdown angles. The spine oscillation is the main mechanism that the model employs in order to reach higher speed, whereas the contribution of touchdown angles is rather minor.

The properties of a representative fixed point corresponding to high velocity bounding were analyzed in detail. The quadrupedal bounding produced in the presence of a linear flexible torso, despite the reduced nature of the model, resembles the motion of galloping mammals and features extended bidirectional spine deformation.

The proposed model also seems promising in terms of energy efficiency due to the extensive spine deformation and the spine-leg coordination. The energetic benefits can be highlighted through a more generic non-dimensional analysis and the incorporation of energy dissipation and torque input.

REFERENCES

[1] M. H. Raibert, *Legged Robots that Balance*. Cambridge, MA: MIT Press, 1986.

[2] www.bostondynamics.com

[3] S. Seok, A. Wang, M. Y. Chuah, D. Otten, J. Lang, and S. Kim, "Design principles for highly efficient quadrupeds and implementation on the MIT cheetah robots," in *Proc. of the IEEE Int. Conference on Robotics and Automation*, Karlsruhe, 2013, pp. 3307–3312.

[4] C. Semini, N. G. Tsagarakis, E. Guglielmino, M. Focchi, F. Cannella and D. G. Caldwell, "Design of HyQ – a Hydraulically and Electrically Actuated Quadruped Robot," in *Proceedings of the Institution of Mechanical Engineers, Part I: Journal of Systems and Control Engineering*, vol. 225, no. 6, 2011, pp. 831-849.

[5] Hutter, M., Remy, C.D., Hoepflinger, M.H., and Siegwart, R., "Efficient and Versatile Locomotion with Highly Compliant Legs", *IEEE/ASME Tran. on Mechatronics*, vol.18, no. 2, 2013, pp. 449-458

[6] R. Blickhan, "The spring-mass model for running and hopping", *Journal of Biomechanics,* vol. 22, no. 11/12, 1985, pp. 1217–1227.

[7] P. Nanua, *Dynamics of a galloping quadruped,* Ph.D. dissertation, Dept. Mech. Eng., Ohio State University, Columbus, 1992.

[8] I. Poulakakis, E. Papadopoulos, and M. Buehler, "On the Stability of the Passive Dynamics of Quadrupedal Running with a Bounding Gait," *The Int. J. of Robotics Research*, v. 25, n. 7, 2006, pp. 669–687.

[9] N. Cherouvim, E. Papadopoulos, "Speed and Height Control for a Special Class of Running Quadruped Robots," in *Proceedings of the IEEE International Conference on Robotics and Automation (ICRA '08),* 2008, Pasadena, CA, pp. 825-830.

[10] M. Hildebrand, "Motions of the running cheetah and horse*", Journal of Mammalogy,* vol. 40, no 4, 1959, pp.481–495.

[11] M. Hildebrand, "Further studies on locomotion of the cheetah", *Journal of Mammalogy* vol. 42, no. 1, 1961, pp. 84–91.

[12] P. E. Hudson, S. A. Corr and A. M. Wilson,"High speed galloping in the cheetah (Acinonyx jubatus) and the racing greyhound, (Canis familiaris): spatio-temporal and kinetic characteristics", *Journal of Experimental Biolog*y, vol. 215, 2012, pp. 2425-2434.

[13] M. Khoramshahi, A. Spröwitz, A.Tuleu, M. N. Ahmadabadi and A. J. Ijspeert, "Benefits of an Active Spine Supported Bounding Locomotion With a Small Compliant Quadruped Robot", in *Proceedings of the IEEE International Conference on Robotics & Automation (ICRA),* Karlsruhe, 2013, pp. 3329–3334.

[14] G. C. Haynes, J. Pusey, R. Knopf, A. M. Johnson and D. E. Koditschek, "Laboratory on Legs: An Architecture for Adjustable Morphology with Legged Robots", in *Proceedings of the SPIE Defense, Security, and Sensing Conference, Unmanned Systems Technology XIV,* 2012.

[15] P. Eckert, A. Sprowitz1, H. Witte and A. J. Ijspeert, "Comparing the effect of different spine and leg designs for a small bounding quadruped robot", in *Proceedings of the IEEE Int. Conference on Robotics & Automation (ICRA),* Seattle, 2015, pp. 3128-3133.

[16] J. E. Seipel, "Analytic-holistic two-segment model of quadruped back-bending in the sagittal plane", in *Proc. of ASME Int. Design Engineering Technical Conferences & Computers and Information in Engineering Conference*, Washington, 2011, pp. 855-861.

[17] Q. Cao, I. Poulakakis, "Quadrupedal bounding with a segmented flexible torso: passive stability and feedback control", *Bioinspiration and Biomimetics,* vol.8, no. 4, 2013.

[18] Q. Deng, S. Wang, X. W., J. Mo, and Q. Liang, "Quasi passive bounding of a quadruped model with articulated spine," *Mechanism and Machine Theory*, vol. 52, 2012, pp. 232–242.

[19] X. Wei, Y. Long, C. Wang and S. Wang, "Rotary galloping with a lock–unlock elastic spinal joint", ," in *Proceedings of the Institution of Mechanical Engineers, Part C: Journal of Mechanical engineering Science*, vol. 225, no. 6, 2014, pp. 1-15

[20] U. Culha and U. Saranli, "Quadrupedal Bounding with an Actuated Spinal Joint," in *Proceedings of the IEEE International Conference on Robotics and Automation*, Shanghai, China, 2011, pp. 1392-1397.

[21] Q. Cao and I. Poulakakis, "Passive quadrupedal bounding with a segmented flexible torso," in *Proceedings of the IEEE/RSJ International Conference on Intelligent Robots and Systems*, Algarve, 2012, pp. 2484–2489.

[22] L. D. Maes, M. Herbin, R. Hackert, V. L. Bels, and A. Abourachid, "Steady locomotion in dogs: Temporal and associated spatial coordination patterns and the effect of speed," *Journal of Experimental Biology*, vol. 211, 2008, pp. 138–149.

[23] N. Schilling and R. Hackert, "Sagittal Spine Movements of Small Therian Mammals during asymmetrical Gaits," *Journal of Experimental Biology*, vol. 209, 2006, pp. 3925–3939.